Available online at www.sciencedirect.com
ScienceDirect
Trans. Nonferrous Met. Soc. China 32(2022) 1188−1204
Transactions of Nonferrous Metals Society of China
www.tnmsc.cn

Grain size effect on cyclic deformation behavior and springback prediction of Ni-based superalloy foil

Wei-lin HE, Bao MENG, Bing-yi SONG, Min WAN

School of Mechanical Engineering and Automation, Beihang University, Beijing 100191, China

Received 27 April 2021; accepted 24 December 2021

Abstract: In order to clarify the influence of grain size on cyclic deformation response of superalloy sheets and springback behavior, cyclic loading−unloading and shearing tests were performed on the superalloy foils with 0.2 mm in thickness and diverse grain sizes. The results show that, the decline ratio of elastic modulus is weakened with increasing grain size, and the Bauschinger effect becomes evident with decreasing grain size. Meanwhile, U-bending test results determine that the springback is diminished with increasing grain size. The Chaboche, Anisotropic Nonlinear Kinematic (ANK) and Yoshida-Uemori (Y-U) models were utilized to fit the shear stress−strain curves of specimens. It is found that Y-U model is sufficient of predicting the springback. However, the prediction accuracy is degraded with increasing grain size.

Key words: grain size effect; cyclic deformation; superalloy foil; hardening model; springback prediction

1 Introduction

Ultrathin-walled superalloy components such as metallic bellow, compact heat exchanger and impingement cooling pipe occupy a considerable proportion in aeroengines and launch vehicles, which play a progressively significant role in structural improvement and performance improvement [1,2]. The wall thickness (t) of these parts is usually between 0.05 and 0.3 mm, which is characterized by the ultrathin-walled workpiece. Due to the advantages of high efficiency, low cost, good material utilization, and desirable workpiece performance, the metal forming has become irreplaceable for mass production of thin-walled components [3,4]. However, the springback occurs easily on the superalloy foil due to its high strength and size affected elastic recovery. Due to the size effect, the cyclic deformation behavior of foil is not consistent with the conventional one. The cyclic deformation behavior of high-strength foils at the micro scale remains unclear, significantly impacting the accuracy of springback compensation and production dimension.

The cyclic deformation behavior and springback of metal foils are found to correlate with the foil thickness and material microstructure. HAOUAOUI et al [5] explored the impact of grain morphology and grain boundary characteristics on Bauschinger effect by multi-pass equal channel angular extrusion on ultrafine-grained copper. They stated that the grain boundary character plays a crucial role in determining the flow stress when the straining is reversed. The dislocation tangle is considered to be favorable in generating back stress. XIANG and VLASSAK [6] obtained the deformation curves of the freestanding copper foils with thicknesses varying from 1.0 to 4.2 μm through plane strain bulge experiment. They concluded that the Bauschinger effect of passivated foils is increased with decreasing film thickness.

Corresponding author: Bao MENG, Tel: +86-10-82338613, E-mail: mengbao@buaa.edu.cn
DOI: 10.1016/S1003-6326(22)65866-7

MAHATO et al [7] discussed the relevance between grain size (d) and Bauschinger effect of annealed copper rod. They pointed out that the back stress is lowered by decreasing grain size because of the strengthened grain boundary obstacles in the small grains. SOHN et al [8] performed the tension−compression experiment on API X80 and X70 steels with the thickness of 14 mm and concluded that the material microstructure and grain size affect the Bauschinger phenomenon. Meanwhile, they argued that the dislocation promotes the Bauschinger effect. FAN et al [9] carried out loading and unloading tensile tests to analyze the cyclic plastic deformation character of pure Mg with diverse grain sizes. They stated that the coarse grain contributes to the apparent reduction of micro strain and elastic modulus.

Recently, the reported literatures focus on the coupled grain size effect, geometrical dimension and the gradient of strain on the springback phenomenon in the micro-bending of metal materials. The micro-bending experiments were conducted on the pure aluminum with diverse thicknesses from 25 to 500 μm by LI et al [10]. The test data revealed that the springback parameters decrease with the increase of material thickness. A simplified plastic strain gradient hardening model was proposed, which can describe the size effects of springback angle. LIU et al [11] analyzed the unloading springback of the 0.1 to 0.6 mm thick pure copper foils after the bending experiments and developed a hardening model to effectively represent the size effect. WANG et al [12] performed the U-bending experiment to explore the size effect on the springback of 0.1, 0.2, and 0.4 mm thick copper alloy foils, and discovered that the size effect contributes more than 90% springback in micro-bending deformation. XU et al [13] conducted V-bending tests of pure copper with diverse thicknesses of 0.1, 0.2 and 0.4 mm and various grain sizes. They demonstrated that the springback angle is reduced when the t/d ratio is decreased. FANG et al [14] used the V-bending test to investigate the impact of t/d ratio on springback of phosphor bronze foil, and they revealed that the foil has the least springback value when t/d =1.

It is seen from the previous literatures that the cyclic deformation behavior and springback of metal foils are significantly affected by size effect. Therefore, the accurate prediction of springback by using diverse constitutive models at different scales is also crucial. In this respect, XU et al [15] developed a kinematic-isotropic hardening model to reflect the softening and cyclic hardening phenomenon. The advantage of the model is that only a set of independent material parameters are required. CHOI et al [16] concluded that Y-U and homogeneity anisotropic hardening (HAH) models can well predict the springback in U-bending. YOSHIDA et al [17] proposed a framework to describe the Bauschinger effect and the plastic anisotropy by supplementing the anisotropic hardening model, which takes the kinematic hardening mechanism into account. In this modeling framework, it is possible to utilize various yielding functions, and the convexity of the yield surface is ensured.

From the above brief review, it is observed that the prediction precision of springback mainly relies on the cyclic plastic deformation mechanism and the constitutive model. However, the materials used in the previous works are generally limited to aluminum alloy, copper and other soft materials. The cyclic deformation behavior of superalloy foils is still obscure. Furthermore, the applicability of existing hardening models under micro-scaled scenarios also needs to be addressed. In the present study, the uniaxial tensile tests, cyclic loading−unloading tests and cyclic shearing tests were performed to reveal the influence of grain size on the monotonous and cyclic deformation response of superalloy foil. In addition, the U-bending test was conducted to analyze the dependence of springback on grain size. Besides, the parameters in the common-used hardening models were identified to evaluate the validity of the macroscopic hardening models at microscale. The findings in this research are useful to accelerate the application of micro-forming technology in the manufacture of ultrathin-walled difficult-to-deform components and improve the forming accuracy via acceptable compensation of springback.

2 Experimental

2.1 Objective material

Superalloys are widely utilized in aerospace, nuclear energy and petroleum industrial clusters because of their high yield strength, superior fatigue

resistance, excellent oxidation and outstanding corrosion resistance. To obtain the impact of grain size on the cyclic deformation behavior of superalloy foil, the Ni-based superalloy GH4169 was selected, and its chemical compositions are illustrated in Table 1. The 0.2 mm-thick superalloy foil was annealed in a vacuum furnace under diverse conditions to obtain diverse grain sizes.

Table 1 Chemical composition of superalloy GH4169 foil (wt.%)

Ni	Cr	Nb	Mo	Ti	Al	C	Fe
52.98	19.55	5.14	3.00	0.92	0.78	0.044	Bal.

After the heat treatment, the chemical etching with the liquor of 10 g/mL mixture of concentrated hydrochloric acid and hydrogen peroxide was utilized to obtain the average grain size. Figure 1 depicts the cross-sectional microstructures at different heating temperatures. The grain size obtained under various heat treatment conditions is summarized in Table 2. It can be seen that the grain size is increased with the increase of heat treatment temperature. According to previous studies [18−22], the dislocation density of the Ni-based superalloy is also decreased with the increase of grain size.

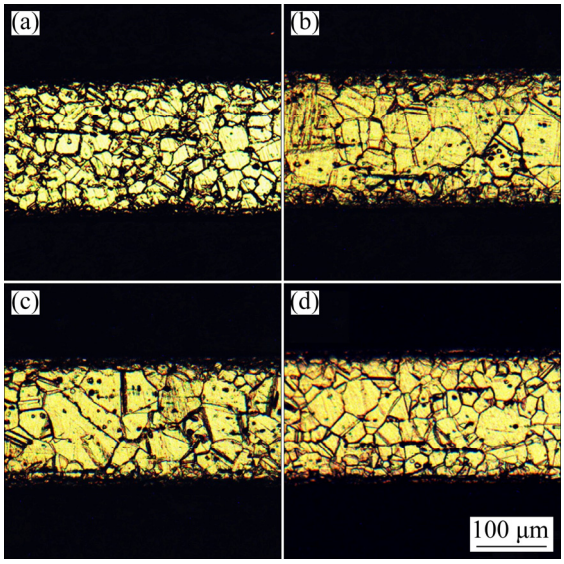

Fig. 1 Microstructures of nickel-based superalloy GH4169 at diverse annealing temperatures: (a) 1000 °C; (b) 1030 °C; (c) 1050 °C; (d) 1100 °C

Table 2 Grain size of superalloy GH4169 under different heat treatment conditions

Thickness/mm	Dwelling time/min	Temperature/°C	Grain size/μm
0.2	20	1000	27.1
0.2	20	1030	41.9
0.2	20	1050	64.9
0.2	20	1100	79.4

2.2 Uniaxial tensile test

The sample with the gauge length of 50 mm and width of 12.5 mm for the uniaxial tensile test was designed. The specimen was fabricated along with three directions, i.e., 0°, 45°, and 90° to the rolling direction. All the tests were operated on an MTS-E44 testing machine at room temperature. The sample was deformed with a specified speed of 5 mm/min until the occurrence of fracture. The strain was recorded via digital image correlation (DIC) technology. Each uniaxial tensile test was conducted at least three times to guarantee the repeatability.

2.3 Cyclic loading−unloading test

To explore the grain size effect on the anelastic behavior of Ni-based superalloy foil, the cyclic loading−unloading test was carried out at room temperature. The deformation velocity was chosen as 5 mm/min. The specimen dimension was the same as that used in the uniaxial tensile test. The strain was recorded by an extensometer with a gauge of 50 mm. Cyclic loading−unloading test consisted of five sequences, including continuous loading to prescribe pre-strain, loading to the set strain interrupt, continuous unloading, unloading to the set stress interrupt, and reloading up to the next pre-strain. The five stages were repeated throughout the test process until the pre-determined maximum strain was reached. The sample was cyclically unloaded and reloaded until pre-strain was 22.5% with a cyclically incremental pre-strain of 1.5% to ensure that the elastic modulus fell to a steady value in each cycle. Each pre-strain represented the true strain of the foil at the beginning of each cycle. To prevent the buckling phenomenon after unloading, reverse loading was initiated when the unloading force reached 30 N. The test was repeated three times for all four grain size materials to ensure the experimental accuracy.

2.4 Cyclic shearing test

Since the large stress level can be achieved, the cyclic shearing test was adopted to elucidate the grain size effect on the cyclic deformation

characteristic of Ni-based superalloy foil and calibrate the material parameters in diverse hardening models. During the cyclic shearing test, the rectangular specimen was firmly clamped by the fixed and moving grips, as illustrated in Fig. 2. The length (l) and width (h) of the shearing zone are 50 mm and 3 mm, respectively. The total width (W) of the specimen is 60 mm. To ensure the simple shearing deformation, the moving grip can only move lengthways. The moving grip was impelled by the load (P) along the y-axis to the pre-set strain. Then, the moving grip moved towards the opposite direction to a certain displacement. To eliminate the connection gap and avoid the slipping of the sample, the first group of screws, i.e., seven M6 mm screws were set at the holding zone. The second group of screws, i.e., six M4 mm screws were arranged at the edge of the deformation zone on both sides to ensure the uniform distribution of plastic strain. To eliminate the sliding between the specimen and the grip, the tightening torques of the two sets of screws were 35 and 5 N·m, respectively. The shearing stress−strain curve under cyclic loading was recorded by the load cell and DIC technology. Different values of pre-strain were set during forwarding shearing for the foils with diverse grain sizes. The pre-strain of the specimen was controlled by displacement. The forward displacement and reverse displacement of the specimen were the same. The displacement values were set to 0.625, 1.125 and 1.5 mm. A total of 12 sets of cyclic shearing tests (four grain sizes × three pre-strain) were performed, and each condition was repeated at least three times.

2.5 U-bending test

To analyze the grain size effect on the springback of superalloy foil and evaluate the feasibility of the macro-scaled hardening models at microscale, the U-bending test was conducted. The geometric dimensions of the test setup were illustrated in Fig. 3. The length and width of the specimen were designed as 110 and 30 mm, respectively, and the length direction was cut from the strip along the rolling direction. The radii of the punch and die were both 3 mm, and the stamping stroke was 28 mm. During the experiment, the sample was deformed at a stationary speed of 10 mm/min with a blank holder force of 5 kN. During the test, the die was fixed, and the blankholder cylinder drove the blankholder to move upward to press the foil. Then, the main oil cylinder drove the punch to move upward to form u-shaped parts. The double-sided polyethylene film lubrication was utilized to improve the lubricating condition at the workpiece/die interface. The test of samples with different grain sizes was repeated 3−8 times until the springback phenomenon was stable. The springback angle was measured via the image processing method, which was captured after the sample was removed from the die.

3 Results and discussion

3.1 Effect of grain size on cyclic deformation behavior

3.1.1 Grain size effect on anelastic behavior

Figure 4 presents deformation responses of the specimens with diverse grain sizes during the cyclic loading−unloading deformation. It is seen that the flow stress is diminished with the grain size increasing, which can be interpreted by the Hall−Petch relation. Furthermore, it is noted that the stress−strain curves do not coincide with each other in the loading and unloading processes, which reflects the nonlinear recovery phenomenon and leads to the emergence of the elastic hysteresis loop. To characterize the recovery phenomenon, the linear and nonlinear methods were usually adopted.

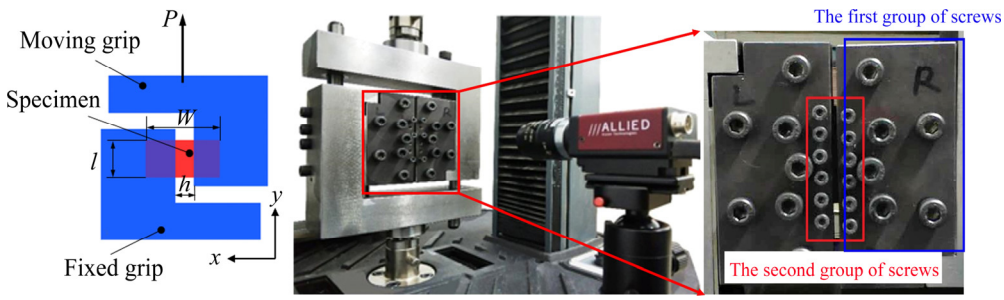

Fig. 2 Schematic of cyclic shearing test

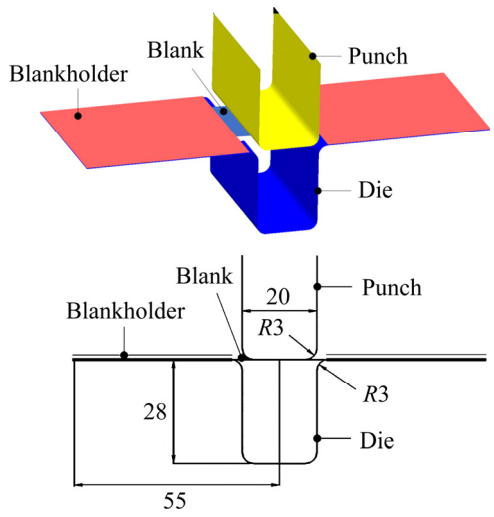

Fig. 3 Geometric dimensions of U-bending setup (Unit: mm)

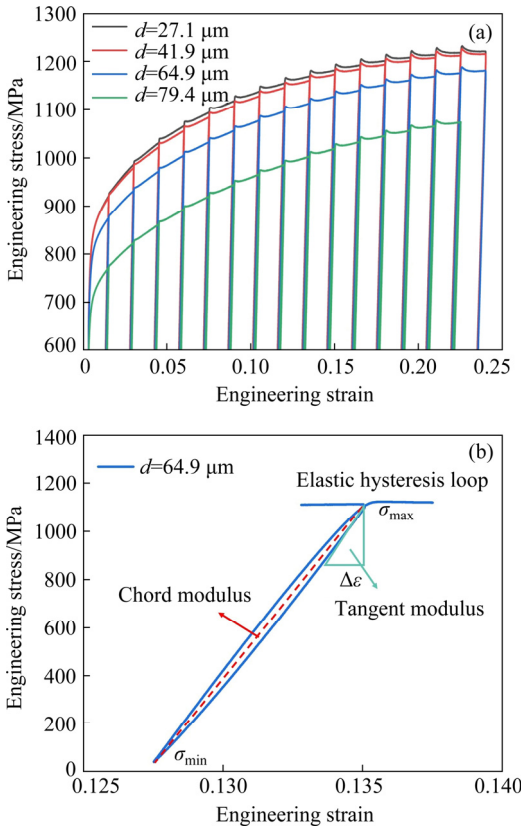

Fig. 4 Anelastic behavior of superalloy foils with different grain sizes: (a) Stress−strain responses in cyclic loading−unloading test with different grain sizes; (b) Definition of chord and tangent moduli

For the linear method, it is necessary to define the chord modulus as the slope of test curve [23]:

$$E_{\text{chord}}=\frac{\sigma_{\max}-\sigma_{\min}}{\varepsilon_{\max}-\varepsilon_{\min}} \tag{1}$$

where E_{chord} stands for the chord modulus, $\sigma_{\max}$ and $\sigma_{\min}$ are the maximum and minimum stress values in elastic hysteresis loop, and $\varepsilon_{\max}$ and $\varepsilon_{\min}$ are the strains corresponding to $\sigma_{\max}$ and $\sigma_{\min}$, respectively. The attenuation of the chord modulus (E_{chord}) is calculated by the following formula proposed by YOSHIDA et al [24]:

$$E_{\text{chord}}=E_{0\text{-c}}-(E_{0\text{-c}}-E_{\text{a}})[1-\exp(-\xi\bar{\varepsilon})] \tag{2}$$

where E_{a} is the chord modulus when plastic strain is infinitely large, which is termed as the saturated modulus; $E_{0\text{-c}}$ is the initial value of chord modulus; ξ determines the decrease rate of chord modulus; $\bar{\varepsilon}$ denotes the equivalent plastic strain, i.e., pre-strain. The fitting curves of chord modulus of various grain sizes are presented in Fig. 5. It is observed that the attenuation formula of chord modulus is still applicable to superalloy foil regardless of grain size. Furthermore, it is found that chord modulus is decreased with growing pre-strain, and the value tends to saturation at a certain strain, which is about 90% of the initial magnitude. This phenomenon is related to the dislocation rearrangement mechanism, damage and crack evolution mechanism and the residual stress mechanism. Due to the strong dependence of springback prediction on the change of chord modulus, it is necessary to take the attenuation of chord modulus into account for precision prediction of springback.

For the nonlinear method, SUN and WAGONER [25] introduced the quasi-plastic−elastic (QPE) model, which divides the nonlinear unloading process into three stages including elastic, classically plastic and transitional stages. The slope of the nonlinear stress−strain behavior is represented as follows:

$$E_{\text{T}}=E_{0\text{-T}}-A_1[1-\exp(-A_2\,|\,\mathrm{d}\varepsilon\,|)] \tag{3}$$

where E_{T} stands for the tangent modulus, $E_{0\text{-T}}$ is the initial value of elastic modulus, A_1 and A_2 are the material parameters, and $|\mathrm{d}\varepsilon|$ is the absolute value of the strain increment during unloading. The fitting results of the tangent modulus under diverse grain sizes are depicted in Fig. 6. It is seen that the tangent modulus can also represent the anelastic behavior of superalloy foil.

To calibrate the effect of grain size on the two types of moduli, the decreasing ratio of two kinds of elastic moduli is calculated, as shown

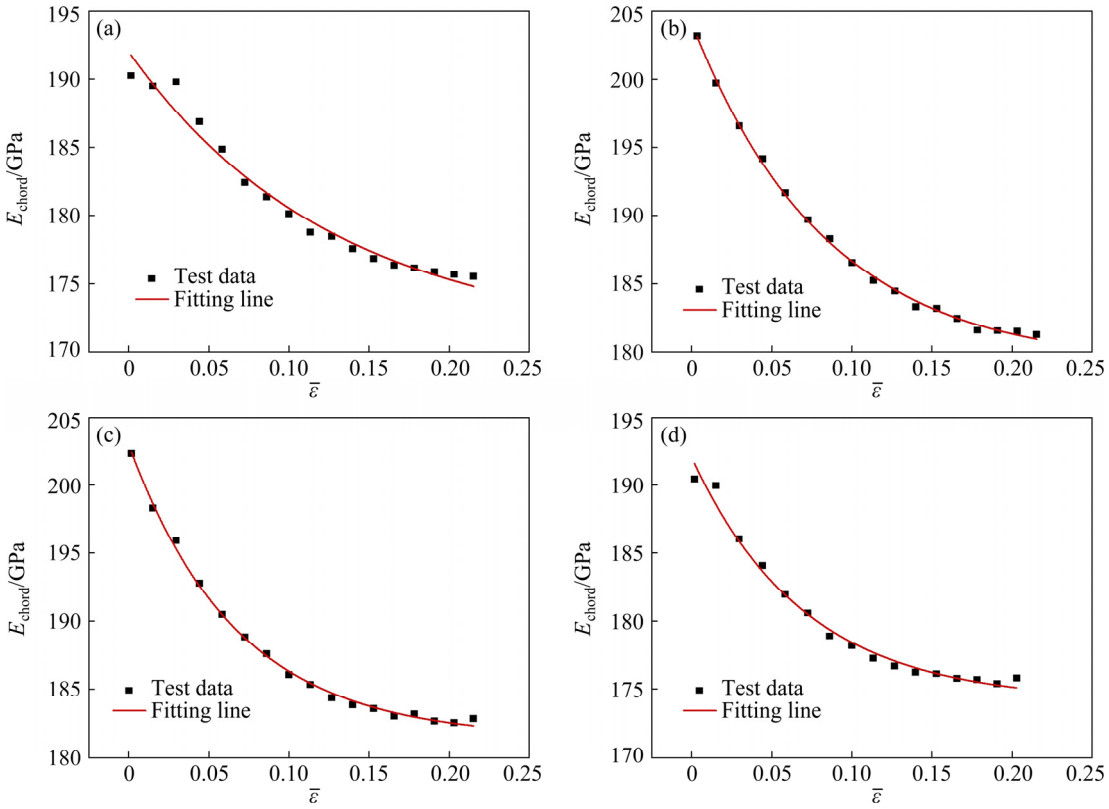

Fig. 5 Relationship between chord modulus and equivalent plastic strain with diverse grain sizes: (a) 27.1 μm; (b) 41.9 μm; (c) 64.9 μm; (d) 79.4 μm

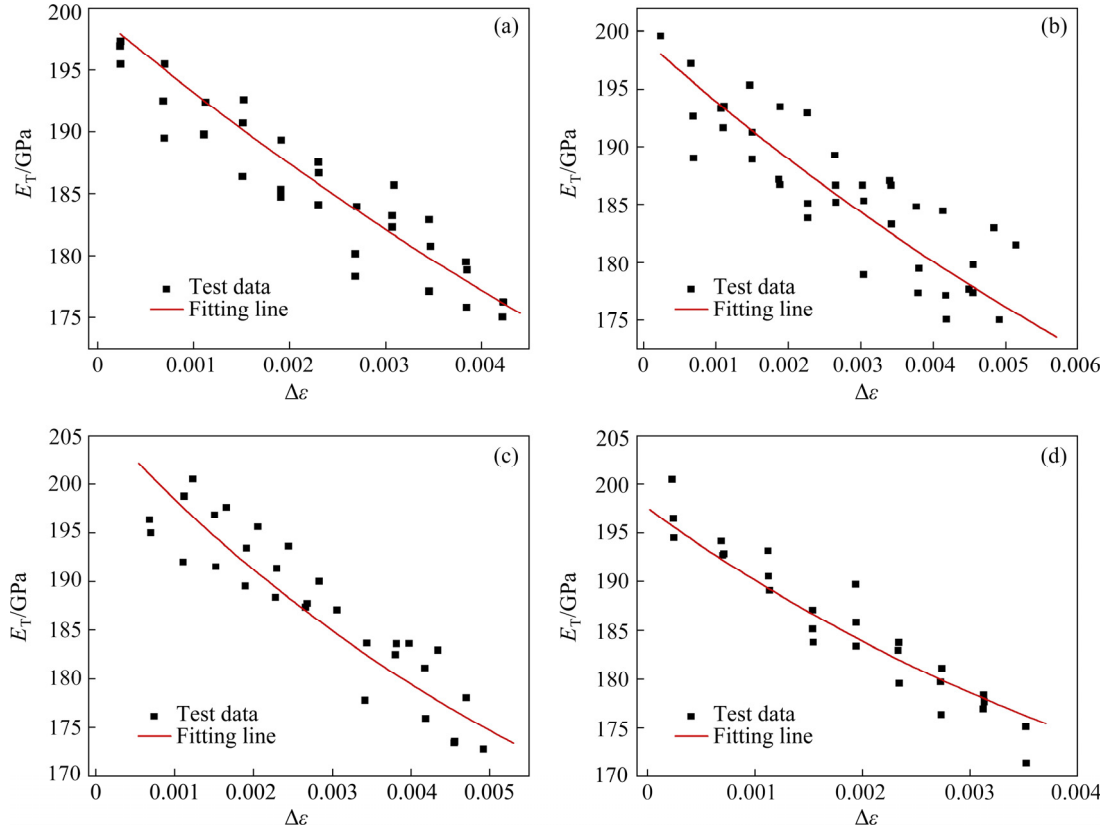

Fig. 6 Relationship between tangent modulus and true strain ($\Delta\varepsilon$) with diverse grain sizes: (a) 27.1 μm; (b) 41.9 μm; (c) 64.9 μm; (d) 79.4 μm

in Fig. 7. E_b(=$E_{0\text{-}T}$−A_1) is the saturation tangent modulus in Fig. 7(b). On the one hand, it can be seen from Fig. 7(a) that the initial value of chord modulus is decreased slightly with the increase of grain size. This is consistent with the findings of GAO et al [18]. On the other hand, it is found that the decline ratios of chord and tangent moduli are decreased with increasing grain size, which can be interpreted by dislocation density theory. The dislocation density is decreased for the coarse-grained specimen, and the attenuation of modulus is related to dislocation. When the external force is eliminated, the dislocation tends to migrate with the internal repulsion, resulting in a reduction in the elastic modulus. With the increasing grain size, the dislocation density is reduced, which causes the attenuation of the decline ratios of the chord and tangent moduli.

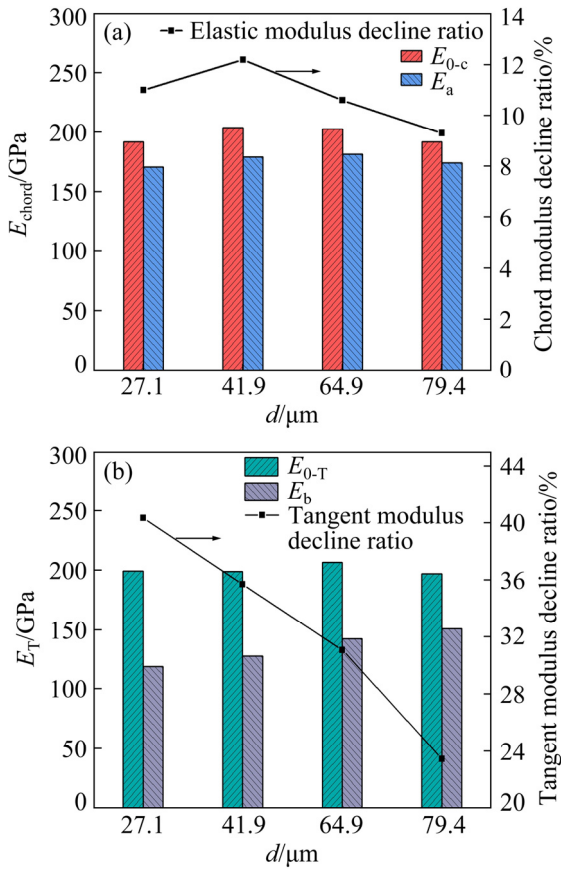

Fig. 7 Grain size effect on elastic modulus: (a) Chord modulus; (b) Tangent modulus

In addition, the decline ratio of chord modulus is related to the elastic hysteresis loop. The elastic hysteresis loop is formed due to the non-coincidence of the loading and unloading deformation, which represents the difference between energy storage under load sequence and energy release in the unloading process. The dissipated energy of each cycle is calculated to explore the grain size effect, as shown in Fig. 8. It can be observed that the dissipated energy is increased with pre-strain, which is closely related to the dislocation pinning. The changing trend agrees well with the findings clarified by SUN and WAGONER [25]. In addition, the fitting slope is decreased with the increasing grain size. The dissipated energy is directly relevant to the internal friction of the foil, which causes the loss of chord modulus. Therefore, the increasing grain size inevitably results in the decrease of chord modulus, which will eventually lead to the decreased decline ratio of chord modulus.

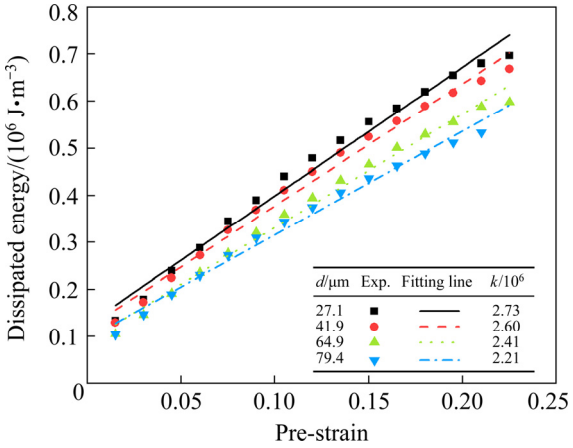

Fig. 8 Relationship among dissipated energy, pre-strain and grain size

3.1.2 Grain size effect on Bauschinger effect

Since the Bauschinger effect plays a significant role in the establishment of cyclic plastic constitutive model and the prediction of springback behavior, its dependence on grain size is explored. To quantify the Bauschinger effect in cyclic shearing test, the softening amount and back stress were utilized. The magnitudes of softening and back stress can represent the degree of the Bauschinger effect. The softening amount ($\Delta\sigma$) and back stress (σ_b) are defined as

$$\Delta\sigma=\sigma_{fs}-\sigma_{rs} \tag{4}$$

$$\sigma_b=\frac{\Delta\sigma}{2} \tag{5}$$

where σ_{fs} is the positive yield stress, and σ_{rs} stands for the reverse yield stress. σ_{fs} and σ_{rs} are the stress values at the finish of the elastic section and the

stress value when the opposite strain is 0.2%, respectively.

According to the stress−strain responses under different grain sizes and pre-strains, Bauschinger parameters are calculated, as presented in Fig. 9. It is observed that the softening value is enlarged with the decrease of grain size, which revealed that the Bauschinger effect is strengthened with the decrease of grain size. This phenomenon can be calibrated by the grain boundary effect and the dislocation density theory.

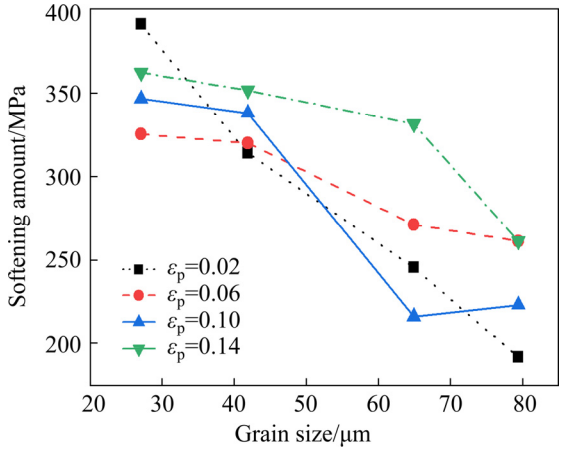

Fig. 9 Relationship among softening amount, pre-strain (ε_p) and grain size

On the one hand, the total boundary of grains becomes smaller with the increase of grain size, which leads to the decrease of the region where micro-stress can appear during the deformation process. Meanwhile, the quantity of grains across the thickness direction is small in coarse-grained foil. Consequently, the dislocation slides out of the free surface through few obstacles and short paths. The rate of dislocation annihilation is aggravated, and the surface layer effect becomes dominant, which eventually results in a decrease in forest dislocation density and flow stress. Therefore, when the coarse-grained sample is deformed in reverse, less obvious Bauschinger effect is observed.

On the other hand, the alter of the Bauschinger effect with grain size can be interpreted by the dislocation density theory, as illustrated in Fig. 10. There are a few dislocations in the material before deformation. When the positive loading initiates, more dislocations appear due to the resolved shear stress, and the dislocations move in stress direction along the glide plane. According to the Kocks−Mecking theory [26], the grain boundaries play a role as barriers to moving dislocation. The moving dislocation within the grain and along the grain boundary would all be piled up at the grain boundary. There is an interaction between the cumulated dislocation and the grain boundary, which results in back stress. During positive loading process, the externally applied stress is required to overcome back stress. Thus, the direction of back stress is regarded as opposite to that of the resolved shear stress. More grain boundaries act as obstacles to dislocations for fine-grained specimen, which induces the intensified back stress. When the external loading becomes reversed, the direction of the resolved shear stress becomes consistent with that of back stress, which leads to a decrease in the reverse shearing stress required to drive the dislocation motion. The reduced value of shearing stress is manifested as the softening amount of stress. For the fine-grained specimen, the grain boundaries and dislocation are more than those in the coarse-grained one. Therefore, the back stress is more tremendous at the grain boundary in fine-grained foil, which causes more pronounced Bauschinger effect.

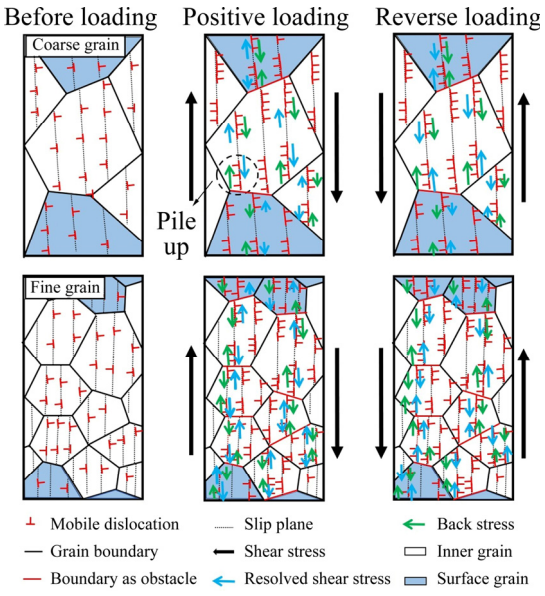

Fig. 10 Mechanism of grain size effect on Bauschinger effect

3.2 Effect of grain size on springback behavior

Figure 11 depicts the impact of grain size on the configuration of the deformed specimens in the U-bending test. In Fig. 11(a), θ_1 is the angle

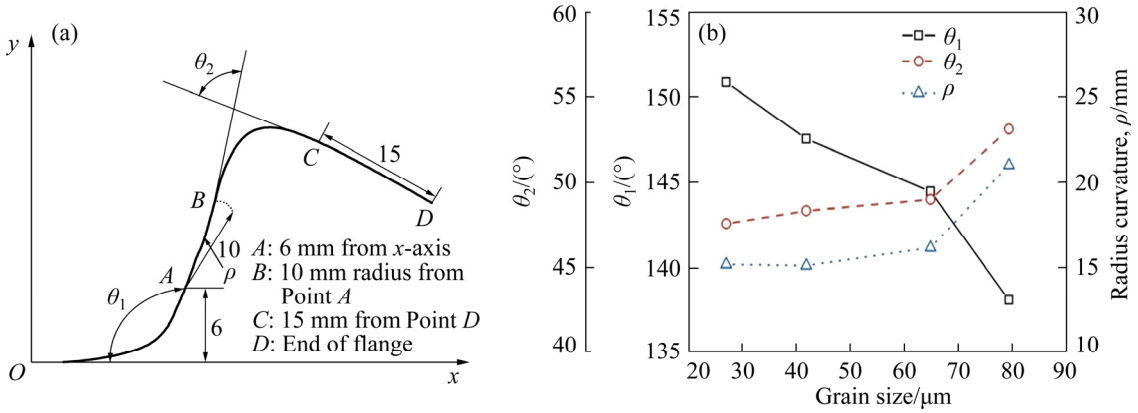

Fig. 11 Effect of grain size on springback: (a) Definition of U-bending springback parameters; (b) Variation of springback parameters under different grain sizes

between x-axis and AB, θ_2 is the angle between AB and CD segments, and ρ is the radius of the circle through AB. Figure 11(b) shows the springback parameters obtained in the U-bending test under various grain sizes. It is noted that the springback becomes evident with decreasing grain size, which is associated with the grain boundary strengthening effect and the surface layer effect.

The whole grain boundary region is reduced for coarse-grained specimen. In the bending process, the dislocation accumulates at the grain boundary with the increase of plastic strain, which leads to an increase in dislocation density. Due to the fact that the flow stress is proportional to the dislocation density according to the Taylor relationship, the flow stress at grain boundary is greater than that inside grain. This phenomenon leads to the stress concentration at the grain boundary and the grain boundary strengthening effect. Thus, large deformation will occur within the grain for the coarse-grained sample due to the small change in the surface state of grain boundary region, which eventually causes less springback in U-bending deformation.

In addition, according to the surface layer model [27], the polycrystalline material is considered to be composed of surface and interior grains. The surface grains have less constraint than the inner ones, which slip and rotate more easily, causing smaller flow stress and easier plastic forming compared to the inner grains. The number of grains in the thickness direction is decreased with increasing grain size, and the proportion of surface grains is thereupon raised. Since springback is mainly induced by the elastic recovery, the superalloy foil with coarse grain produces a larger plastic deformation zone, which leads to less springback.

3.3 Effect of grain size on prediction accuracy of springback

3.3.1 Parameter identification in hardening model

The hardening model reflects the strengthening behavior of metal material during cyclic plastic deformation. The prediction of springback is directly related to the validity of the used hardening models. To evaluate the common-used hardening models under diverse grain sizes, the Chaboche, ANK and Y-U models were utilized to fit the deformation curves of the specimens subjected to cyclic shearing deformation. CHABOCHE and ROUSSELIER [28] developed the Chaboche model by decomposing the back stress into multiple components, which still conforms to the A-F model [29]. The ANK model was presented by CHUN et al [30] to describe the evolution of back stress in reverse loading and better reflect Bauschinger effect. The Y-U hardening model [31] is based on a hyperboloid frame and consists of a yielding and a boundary surface. The yielding surface shifts within the boundary surface. Besides, an additional surface followed by a kinematic hardening model is introduced to reflect the work hardening stagnation phenomenon according to the position relationship between the boundary and additional surfaces.

In this research, the adaptive simulated annealing (ASA) algorithm was used to solve parameters in the Chaboche and Y-U models. The algorithm was conducted by using ls-opt and

ls-dyna platforms. Whereas, the parameters of the ANK model were obtained by using the global optimization algorithm. The solved parameters of three models are displayed in Tables 3, 4 and 5. Here, Y represents the radius of the yield, B is the original size of bounding surface, k controls the isotropic hardening rate, b represents isotropic hardening parameter, R_{sat} is the saturated magnitude of the isotropic hardening stress when strain is infinity, C governs the speed of the kinematic hardening, and h describes the hardening stagnation behavior. In Table 4, σ_0 is the initial yield stress, C_{Cha} is the initial subsequent hardening modulus, γ represents the variation speed of C_{Cha} with plastic deformation, and H is the isotropic plastic hardening modulus. As for the ANK model, σ_{ANK} is the initial yield stress, b_{ANK}, Q, γ_1 C_1 and C_2 represent the material hardening parameters.

3.3.2 Comparison of different hardening models

Figure 12 displays the fitting result of cyclic stress−strain behavior using different hardening models under diverse grain sizes. In the forward loading process, both three models have good fitting accuracy for the elastic deformation stage. However, the prediction via Chaboche model deviates from the experimental data for the plastic deformation stage when the grain sizes are 27.1 and 64.9 μm. Meanwhile, the maximum pre-strains fitted by Chaboche model are lower than the experimental results. On the other hand, the prediction of Chaboche and ANK models are failed to reflect the instantaneous softening phenomenon in cyclic deformation of superalloy foil. Comparing with Y-U model, neither of the two models contains material parameters to describe instantaneous softening behavior. In addition, the permanent softening phenomenon obtained by Chaboche model deviates from the experimental curves, and the predicted softening amount is less than the test result. These deviations are due to the fact that the Chaboche model only includes parameters describing the kinematic hardening mechanism. On the contrary, when the strain in the reverse loading stage is less than zero, the prediction value of permanent softening stage by ANK model is significantly higher than the experimental result. This is because back stress evolution in the reverse section mainly considers the situation where the strain is greater than zero in ANK model. When the strain is less than zero, the precision of the model is naturally decreased. On the contrary, the fitting results of Y-U model are consistent with test results.

Table 3 Parameters of Y-U model under different grain sizes

Grain size/μm	Y/MPa	B/MPa	k	b/MPa	R_{sat}/MPa	C	h
27.1	779.496	903.924	5.89723	131.901	537.442	94.9794	0.589068
41.9	723.776	874.49	3.88556	160.279	669.709	103.479	0.520749
64.9	653.401	780.212	3.84727	159.507	754.039	137.301	0.400029
79.4	627.975	740.862	1.83337	197.906	1386.5	97.0193	0.482643

Table 4 Parameters of Chaboche model under different grain sizes

Grain size/μm	σ_0/MPa	C_{Cha}	H	γ
27.1	829.582	13065.4	839.016	46.9762
41.9	809.572	6432.9	1049.34	27.9751
64.9	775.133	6430.28	1054.44	29.2296
79.4	693.113	5999.58	1254.93	33.3056

Table 5 Parameters of ANK model under different grain sizes

Grain size/μm	b_{ANK}/MPa	Q/MPa	γ_1	C_1/MPa	C_2/MPa	σ_{ANK}/MPa
27.1	13.91	530.7	38.21	6163	124	782
41.9	12.84	504.9	29.83	3715	161	760.8
64.9	10.17	551.4	27.81	2514	147	703.2
79.4	6.76	611.5	6.85	602.9	134	680.5

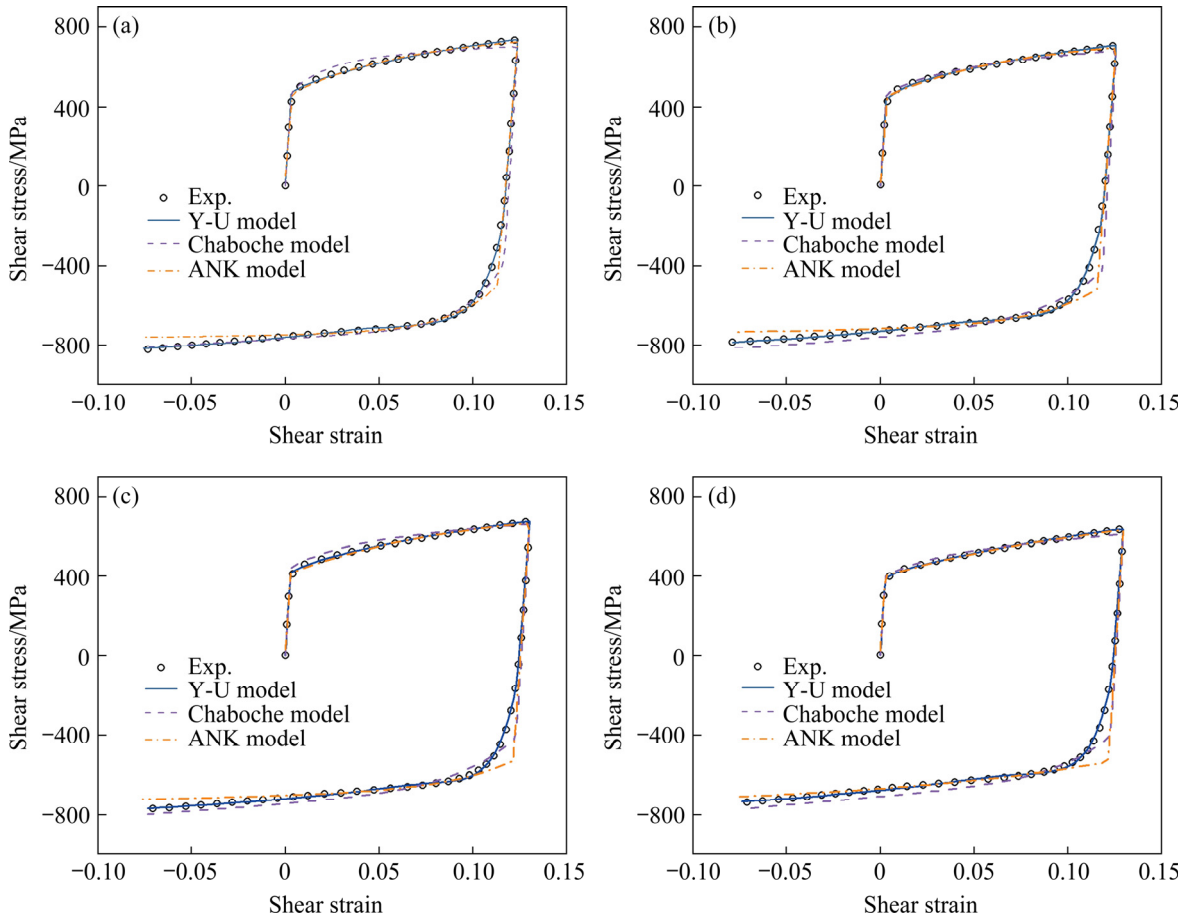

Fig. 12 Fitting results of different hardening models with diverse grain sizes: (a) 27.1 μm; (b) 41.9 μm; (c) 64.9 μm; (d) 79.4 μm

Due to the additional surface introduced in the Y-U model that can fit experimental results flexibly and smoothly, the Y-U model is utilized to further analyze and explore the effect of grain size on the prediction accuracy of springback.

3.3.3 Effect of grain size on accuracy of Y-U hardening model

The fitting precision of Y-U hardening model can reflect the grain size effect on springback prediction. Since the cyclic deformation curve drawn by the utilization of the parameters obtained from multiple pre-strains is closer to the experimental one, the following analysis is based on the parameters in Y-U model obtained by fitting cyclic curves under three pre-strains. The fitting results of Y-U model under diverse grain sizes are shown in Fig. 13. It is seen that the fitting curve confirms the experimental data. Nevertheless, the fitting result in some regions slightly deviates from the experimental one with the increasing grain size, which indicates that the prediction accuracy of Y-U hardening model is weakened with the increasing grain size.

To investigate the effect of grain size on the validity of the Y-U model, the sum of the root mean square deviations (RMSD) for forward and reverse loading of each cyclic curve is calculated. The mean RMSD of the three loops under different grain sizes is displayed in Fig. 14. It is seen that the RMSD is aggravated with the increasing grain size, which mirrors that the fitting accuracy is shifted down for the coarse-grained superalloy foil. The deformation behavior of individual grain is dominant for the coarse-grained specimen. When the grain size increases but the foil thickness remains unchanged, the properties of individual grain significantly affect the overall material deformation response, which eventually results in the inconsistent mechanical behavior with the macroscopic scenario. Therefore, the multiscale hardening model considering the transformation of deformation mechanism is urgently needed to accurately predict the springback at microscale.

To further elucidate the influence of grain size

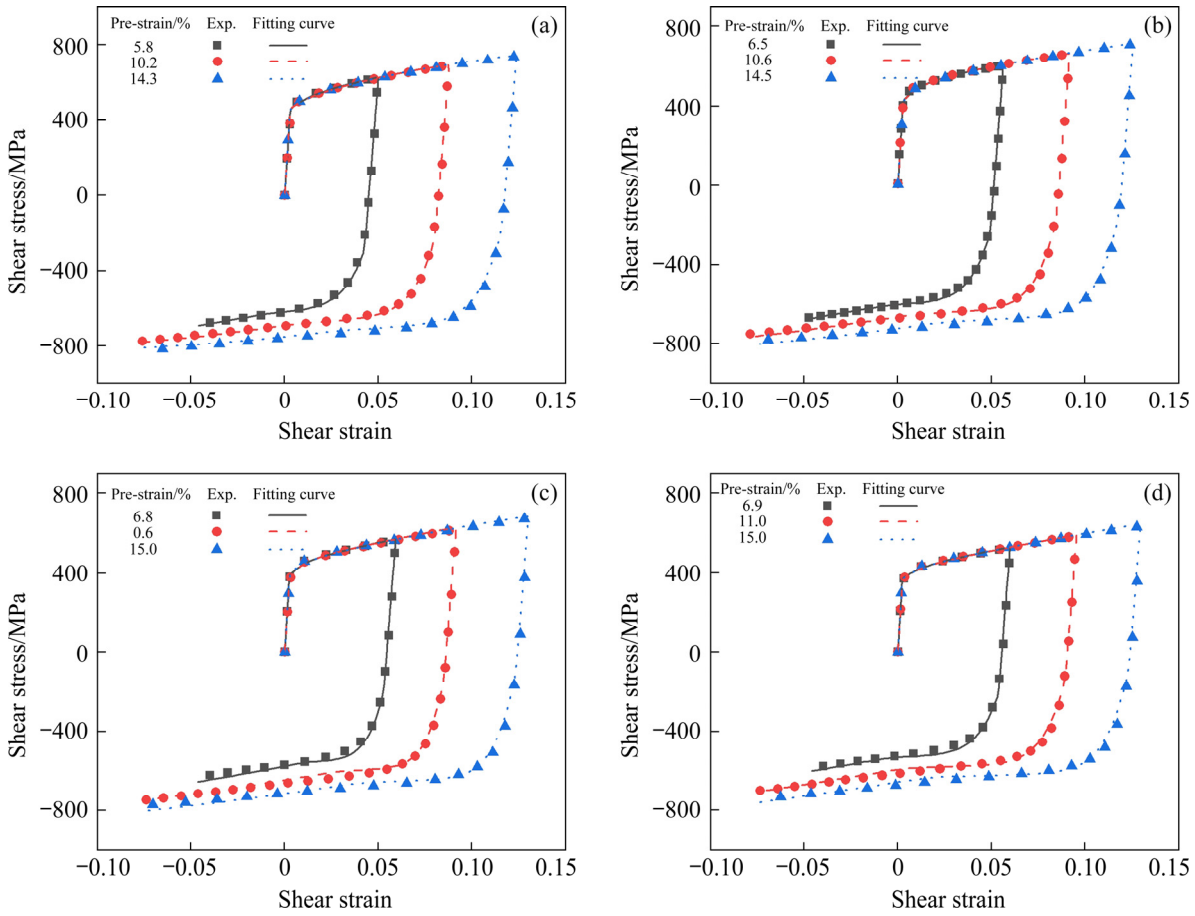

Fig. 13 Fitting results of Y-U model with diverse grain sizes: (a) 27.1 μm; (b) 41.9 μm; (c) 64.9 μm; (d) 79.4 μm

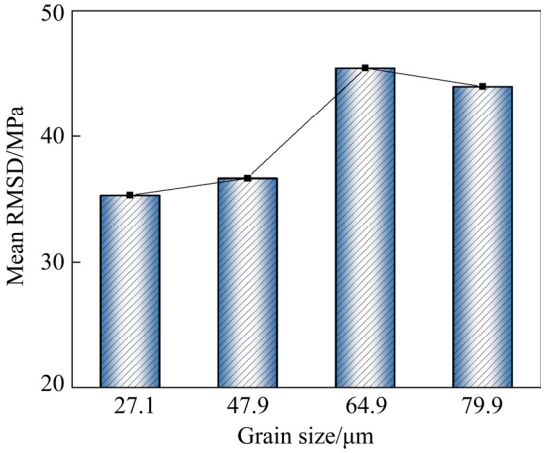

Fig. 14 Mean RMSD with different grain sizes

on fitting accuracy of Y-U model, the dependence of material parameters on grain size was explored, and some evolution trends are similar to the results obtained by JULSRI et al [32]. In Fig. 15(a), the parameter Y conforms to the Hall−Patch equation, which represents the material yield behavior. Compared with coarse-grained foil, fine-grained foil has greater deformation resistance. This is because with the increase of grain size, the proportion of grain boundary is decreased and the surface layer effect becomes more obvious. Furthermore, the volume fraction of different phases of superalloy also affects cyclic plastic deformation behavior of the material. However, the relationship between parameter Y and grain size shows that the flow behavior of superalloy foils with different grain sizes accords with the Hall−Patch equation. It is illustrated that the change of strengthening phase is not obvious after heat treatment and it is reasonable to consider only the effect of grain size on the properties of superalloy foil. Figure 15(b) plots the linear relation between the parameter B and grain size, which demonstrates that the stress level under positive and negative loading is linearly decreased with the increasing grain size. This tendency agrees well with the trend that the flow stress is decreased with the increase of grain size in the uniaxial tensile test. The number of grains in the thickness direction is decreased with the increase of grain size. This makes the dislocation slide out of the free surface through fewer obstacles and shorter paths, which leads to

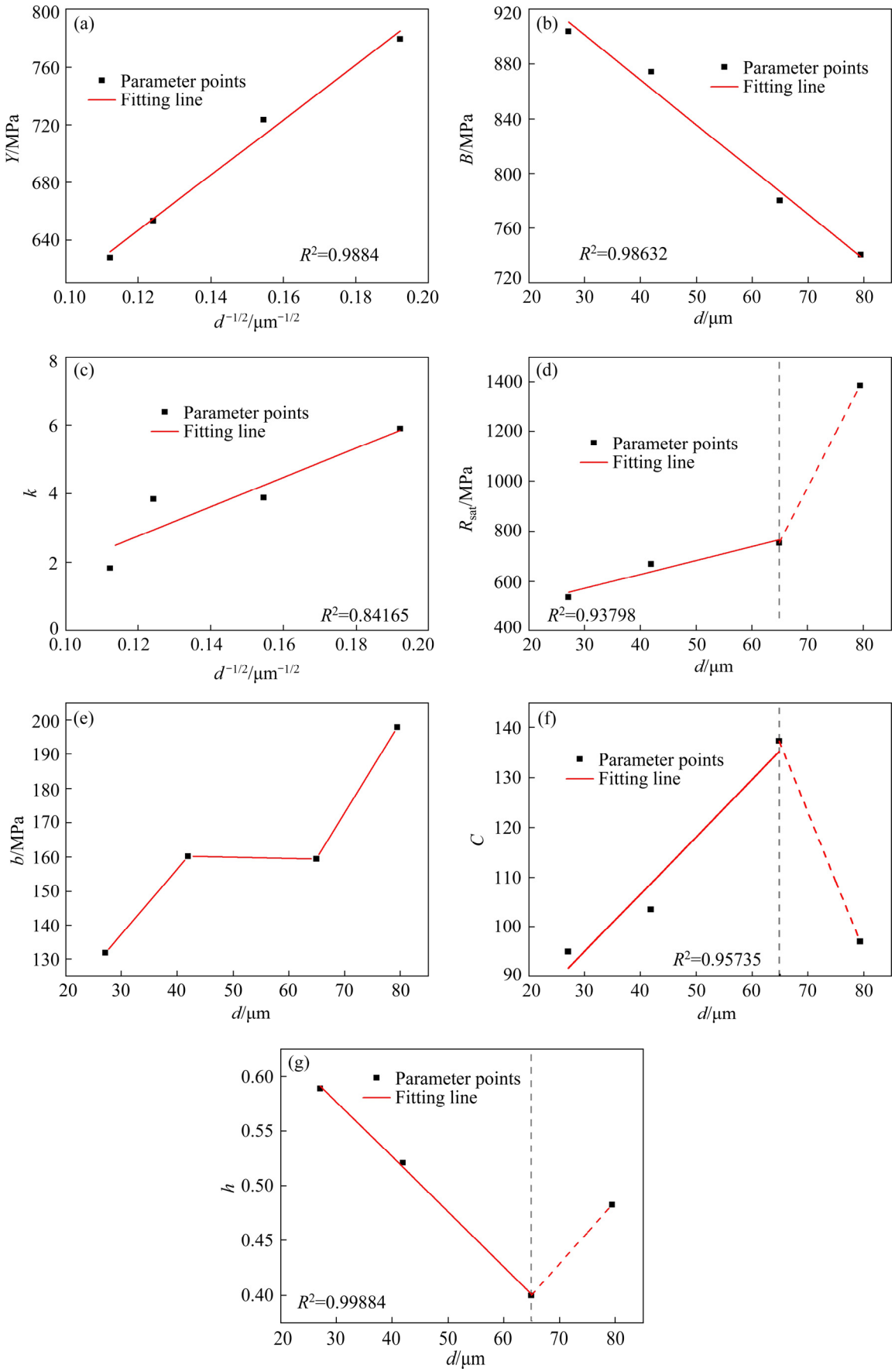

Fig. 15 Grain size effect on material parameters in Y-U model: (a) Y; (b) B; (c) k; (d) R_{sat}; (e) b; (f) C; (g) h

faster dislocation disappearance rate. The foil surface effect becomes more obvious. Finally, the forest dislocation density inside the foil is decreased, and the flow stress is decreased, which is manifested as the decrease of the boundary surface. It can be inferred that the parameter B is related to the change of flow stress.

In addition, the parameter k in Y-U model controls the rate of isotropic and subsequent strengthening. With the increase of k, the stress tends to reach saturation value more quickly and approaches isotropic strengthening. With the grain size increasing, the dislocation density is decreased, and the average free path of dislocation is thereupon increased, leading to the decrease of parameter k, as illustrated in Fig. 15(c). It could be further seen that there is a linear relationship between the parameters k and $d^{-1/2}$. However, the linearity becomes less obvious with the increasing grain size, which shows that grain size influences the strengthening rate of foils, and the extent is changed with the increasing grain size.

In addition, some parameters show peculiar relationship with grain size. Parameters R_{sat} and b affect the bounding surfaces of isotropic hardening and kinematic hardening, respectively. It can be found from Fig. 15(d) that the isotropic saturation stress increases linearly with the increase of grain size. However, when the grain size reaches 79.4 μm, R_{sat} is sharply increased. This is because that with the increase of grain size, a single grain plays a larger role in the superalloy foils, which causes the anisotropy of the foil to become significant. Due to the decrease of grain boundary area, the strain usually occurs inside the grain. The evolution law is inconsistent with that of polycrystalline material. On the other hand, the permanent softening degree of the material is mainly affected by kinematic hardening. Parameter b reflects the degree of permanent softening, which is increased with the increase of grain size, as shown in Fig. 15(e). KIM et al [21] proposed that permanent softening is related to the back stress generated during cyclic loading of the material, but the influencing mechanism needs to be further explored.

Parameter C only affects the hardening rate of the material in the instantaneous softening process in the reverse loading process, but does not affect the flow stress of the material after the instantaneous softening. It is seen from Fig. 15(f) that the parameter C increases linearly with the increasing grain size. This illustrates that the instantaneous softening rate is increased with increasing grain size because the dislocation density of the sample decreases, and the sample is more prone to dislocation slip with the increasing grain size. However, when the grain size is 79.4 μm, the instantaneous softening rate is suddenly decreased because the instantaneous softening rate is closely related to the unstable dislocation motion, such as piled-up dislocations. With the increase of grain size, the material changes from polycrystalline to single crystal [21], and the unstable dislocation motion is decreased, leading to the abrupt shift in softening rate.

Similarly, the parameter h is decreased linearly with the increasing grain size as displayed in Fig. 15(g). It reflects that the process of work hardening stagnation will shorten gradually with the increasing grain size. The process of work hardening stagnation is related to the saturation degree of back stress during deformation [33]. During the transition from transient softening to permanent softening, new dislocations may occur inside the material [21]. The grain boundary area is decreased with the increasing grain size. The newly generated dislocation density is also decreased, resulting in the reduction of the back stress. Therefore, the work hardening stagnation stage of coarse-grained material is short, i.e., the decrease of parameter h. However, the tendency is changed for grain size of 79.4 μm. This abnormal phenomenon indicates that the Y-U model has error in capturing the work-hardening phenomenon of the superalloy foils containing few grains.

To further analyze the validity of Y-U model at different grain sizes, the FE simulation was conducted by using Y-U hardening model to predict the springback of 0.2 mm-thick superalloy foils with diverse grain sizes subjected to the U-bending deformation on Dynaform platform. The Hill'48 yield criterion was adopted in the FE simulation. The anisotropy parameters calculated through the uniaxial tensile test are shown in Table 6. In the FE simulation, the friction coefficient between the mold and the specimen was set at 0.125. The unit type was full integral unit 16. The mesh size of the mold was 1 mm, and the mesh size of the specimen was 0.5 mm. The simulation conditions were consistent with the experimental conditions of

Table 6 Anisotropic parameters in Hill'48 for superalloy GH4169 foil

d/μm	r_0	r_{45}	r_{90}	r_n
27.1	0.8158	0.9201	0.9185	0.8943
41.9	0.8035	0.9145	0.9211	0.8884
64.9	0.8211	0.9123	0.9092	0.8887
79.4	0.8135	0.9024	0.9193	0.8844

U-bending test. Two kinds of material models considering the attenuation of elastic modulus (E) and keeping the elastic modulus constant were adapted. The simulation results were compared with the U-bending test, and the deviations of three springback parameters under different conditions are depicted in Fig. 16. The prediction deviations of the three springback parameters are relatively small, which indicated that the Y-U model is adequate to predict the springback of superalloy foil. However, it is found that the simulation results considering the attenuation of elastic modulus are more approximate to the experimental data, which mirrors that it is necessary to consider the change of elastic modulus in springback prediction. Meanwhile, it is also observed that the deviation is enhanced with increasing grain size, which reveals that the change of grain size impacts the feasibility of Y-U model. As a commonly-used hardening model, the Y-U model does not consider the grain size effect. However, the springback of superalloy foil is affected by the grain size. It is speculated that the prediction accuracy of Y-U model is inevitably worsened when few grains are participating in the deformation. Thus, the influence mechanism of grain size on cyclic deformation behavior should be focused on. In addition, it can be seen that the impact of grain size on the deviation of parameter θ_1 is less than the elastic modulus. In contrast, the grain size effect on parameters θ_2 and ρ is more obvious than the elastic modulus. On the one hand, the material at the corner of the punch is subjected to bending and unloading during the forming process. Consequently, parameter θ_1 reflects the effect of uniaxial tensile and unloading elastic modulus. The relationship between θ_1 and the hardening model which mainly reflects the cyclic plastic behavior is not apparent. The grain size primarily affects the precision of hardening model. Therefore, the prediction accuracy of θ_1 is mainly influenced by the elastic modulus. On the other hand, the material at the side wall undergoes cyclic loading, and parameters θ_2 and ρ are influenced by the hardening model and grain size rather than the elastic modulus. Hence, both the attenuation of elastic modulus and grain size effect should be considered to improve the prediction accuracy.

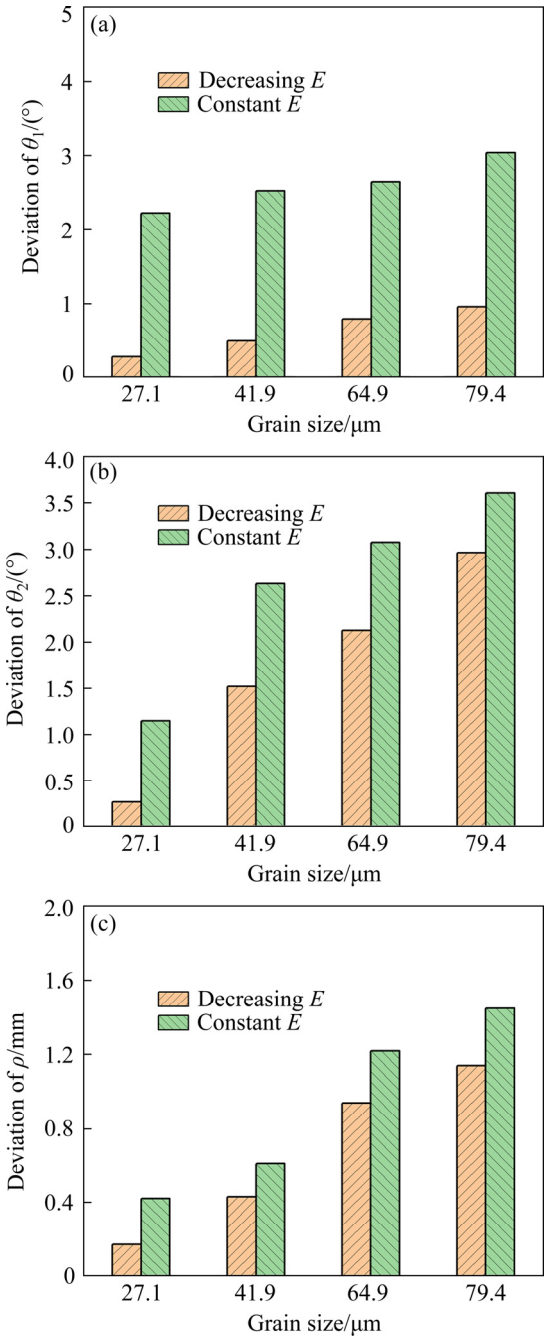

Fig. 16 Effect of grain size on prediction accuracy of Y-U model in U-bending test: (a) θ_1; (b) θ_2; (c) ρ

4 Conclusions

(1) The attenuation of elastic modulus can be represented by chord and tangent moduli, and the attenuation ratio of elastic modulus is decreased

with the increase of grain size. The initial value of the chord modulus is decreased with the increase of grain size. The value of the saturated chord modulus is approximately 90% of the initial value, which is associated with energy dissipation.

(2) The Bauschinger effect is strengthened with the reduction of grain size, which is ascribed to the increase in grain boundaries, back stress and dislocation density.

(3) The Y-U model is preferred over the Chaboche and ANK models to reflect the cyclic deformation behavior of superalloy foil. However, the fitting accuracy is reduced with increasing grain size, and the material parameters are depended on grain sizes.

(4) The Y-U model can accurately predict the springback in U-bending of superalloy foil; however, the fitting accuracy is affected by the combination of attenuation of elastic modulus and grain size.

Acknowledgments

The authors deeply acknowledge the funding support to this research from the National Natural Science Foundation of China (Nos. 51975031, 52075023, 51635005), and Defense Industrial Technology Development Program, China (No. JCKY2018601C207).

References

[1] MENG B, WAN M, ZHAO R, ZOU Zheng-ping, LIU Huo-xing. Micromanufacturing technologies of compact heat exchangers for hypersonic precooled airbreathing propulsion: A review [J]. Chinese Journal of Aeronautics, 2021, 34: 79−103.

[2] QUAN Guo-zhen, ZHANG Yu-qing, ZHANG Pu, MA Yao-yao, WANG Wei yong. Correspondence between low-energy twin boundary density and thermal-plastic deformation parameters in nickel-based superalloy [J]. Transactions of Nonferrous Metals Society of China, 2021, 31(2): 438−455.

[3] FU M W, CHAN W L. A review on the state-of-the-art microforming technologies [J]. The International Journal of Advanced Manufacturing Technology, 2013, 67(9−12): 2411−2437.

[4] MA Zhen-wu, PENG Xuan, WANG Chun-ju, CAO Zi-yang. Modeling of material deformation behavior in micro-forming under consideration of individual grain heterogeneity [J]. Transactions of Nonferrous Metals Society of China, 2020, 30: 2994−3005.

[5] HAOUAOUI M, KARAMAN I, MAIER H J. Flow stress anisotropy and Bauschinger effect in ultrafine grained copper [J]. Acta Materialia, 2006, 54: 5477−5488.

[6] XIANG Y, VLASSAK J J. Bauschinger and size effects in thin-film plasticity [J]. Acta Materialia, 2006, 54: 5449−5460.

[7] MAHATO J K, DE P S, SARKAR A, KUNDU A, CHAKRABORTI P C. Effect of deformation mode and grain size on Bauschinger behavior of annealed copper [J]. International Journal of Fatigue, 2016, 83: 42−52.

[8] SOHN S S, HAN S Y, SHIN S Y, BAE J H, LEE S. Effects of microstructure and pre-strain on Bauschinger effect in API X70 and X80 linepipe steels [J]. Metals and Materials International, 2013, 19: 423−431.

[9] FAN G D, ZHENG M Y, JU C H, HU X S, WU K, GAN W M, BROKMEIER H G. Effect of grain size on cyclic microplasticity of ECAP processed commercial pure magnesium [J]. Journal of Materials Science, 2013, 48: 1239−1248.

[10] LI H Z, DONG X H, SHEN Y, DIEHL A, HAGENAH H, ENGEL U, MERKLEIN M. Size effect on springback behavior due to plastic strain gradient hardening in microbending process of pure aluminum foils [J]. Materials Science and Engineering A, 2010, 527: 4497−4504.

[11] LIU J G, FU M W, LU J, CHAN W L. Influence of size effect on the springback of sheet metal foils in micro-bending [J]. Computational Materials Science, 2011, 50: 2604−2614.

[12] WANG Ji-lai, FU Ming-wang, RAN Jia-qi. Analysis of the size effect on springback behavior in micro-scaled u-bending process of sheet metals [J]. Advanced Engineering Materials, 2014, 16: 421−432.

[13] XU Z T, PENG L F, BAO E Z. Size effect affected springback in micro/meso scale bending process: Experiments and numerical modeling [J]. Journal of Materials Processing Technology, 2018, 252: 407−420.

[14] FANG Z, JIANG Z Y, WANG X G, ZHOU C L, ZHAO X M, ZHANG X M, WU D. Effect of grain size on springback and system energy in micro V-bending with phosphor bronze foil [J]. Metallurgical and Materials Transactions A, 2016, 47: 488−493.

[15] XU L Y, NIE X, FAN J S, TAO M X, DING R. Cyclic hardening and softening behavior of the low yield point steel BLY160: Experimental response and constitutive modeling [J]. International Journal of Plasticity, 2016, 78: 44−63.

[16] CHOI J, LEE J, BONG H J, LEE M G, BARLAT F. Advanced constitutive modeling of advanced high strength steel sheets for springback prediction after double stage U-draw bending [J]. International Journal of Solids and Structures, 2018, 151: 152−164.

[17] YOSHIDA F, HAMASAKI H, UEMORI T. Modeling of anisotropic hardening of sheet metals including description of the Bauschinger effect [J]. International Journal of Plasticity, 2015, 75: 170−188.

[18] GAO Y B, DING Y T, LI H F, DONG H B, ZHANG R Y, LI J, LUO Q S. Grain-size dependent elastic-plastic deformation behaviour of Inconel 625 alloy studied by in-situ neutron diffraction [J]. Intermetallics, 2021, 138: 107340.

[19] LIU Y Z, WAN M, MENG B. Multiscale modeling of coupling mechanisms in electrically assisted deformation of

ultrathin sheets: An example on a nickel-based superalloy [J]. International Journal of Machine Tools and Manufacture, 2021, 162: 103689.
[20] ZHANG P, WANG H, WANG C J, ZHU Q, CHEN G. Explanation of the size effect on the flow stress of thin sheet based on the size of dislocation cell [J]. Materials Science and Engineering A, 2019, 766: 138331.1−138331.6.
[21] KIM J H, KIM D, BARLAT F, LEE M G. Crystal plasticity approach for predicting the Bauschinger effect in dual-phase steels [J]. Materials Science and Engineering A, 2012, 539: 259−270.
[22] KELLER C, HUG E. Kocks-Mecking analysis of the size effects on the mechanical behavior of nickel polycrystals [J]. International Journal of Plasticity, 2017, 98: 106−122.
[23] HASSAN H, MAQBOOL F, GÜNER A, HARTMAIER A, BEN KHALIFA N, TEKKAYA A E. Springback prediction and reduction in deep drawing under influence of unloading modulus degradation [J]. International Journal of Material Forming, 2016, 9(5): 619−633.
[24] YOSHIDA F, UEMORI T, FUJIWARA K. Elastic–plastic behavior of steel sheets under in-plane cyclic tension–compression at large strain [J]. International Journal of Plasticity, 2002, 18(5/6): 633−659.
[25] SUN L, WAGONER R H. Complex unloading behavior: Nature of the deformation and its consistent constitutive representation [J]. International Journal of Plasticity, 2011, 27: 1126−1144.
[26] KOCKS U F, MECKING H. Physics and phenomenology of strain hardening: The FCC case [J]. Progress in Materials Science, 2003, 48: 171−273.
[27] ENGEL U, ECKSTEIN R. Microforming — From basic research to its realization [J]. Journal of Materials Processing Technology, 2002, 125/126: 35−44.
[28] CHABOCHE J L, ROUSSELIER G. On the plastic and viscoplastic constitutive equations—Part I: Rules developed with internal variable concept [J]. Journal of Pressure Vessel Technology, 1983, 105(2): 153−158.
[29] FREDERICK C O, ARMSTRONG P J. A mathematical representation of the multiaxial Bauschinger effect [J]. Materials at High Temperatures, 2007, 24(1): 1−26.
[30] CHUN B K, JINN J T, LEE J K. Modeling the Bauschinger effect for sheet metals, part I: Theory [J]. International Journal of Plasticity, 2002, 18: 571−595.
[31] YOSHIDA F, UEMORI T. A model of large-strain cyclic plasticity describing the Bauschinger effect and workhardening stagnation [J]. International Journal of Plasticity, 2002, 18: 661− 686.
[32] JULSRI W, SURANUNTCHAI S, UTHAISANGSUK V. Study of springback effect of AHS steels using a microstructure based modeling [J]. International Journal of Mechanical Sciences, 2018, 135: 499−516.
[33] RAUCH E F, GRACIO J J, BARLAT F. Work-hardening model for polycrystalline metals under strain reversal at large strains [J]. Acta Materialia, 2007, 55: 2939−2948.

晶粒尺寸对镍基高温合金箔材循环变形行为及回弹预测的影响

贺炜林，孟 宝，宋炳毅，万 敏

北京航空航天大学 机械工程及自动化学院，北京 100191

摘 要：为了探究晶粒尺寸对高温合金箔材循环变形行为和回弹的影响，对厚度为 0.2 mm、不同晶粒尺寸的高温合金箔材进行循环加载−卸载实验和剪切实验。结果表明，弹性模量衰减率随着晶粒尺寸的增大而减小，包辛格效应随着晶粒尺寸的减小变得显著。同时，U 形弯曲试验结果表明，回弹随着晶粒尺寸的增大而减小。采用 Chaboche 模型、ANK 模型和 Yoshida-Uemori(Y-U)模型拟合试样的剪切应力−应变曲线，发现 Y-U 模型是预测回弹的有效模型，然而，随着晶粒尺寸的增大，模型预测精度有所降低。

关键词：晶粒尺寸效应；循环变形；高温合金箔材；强化模型；回弹预测

(Edited by Xiang-qun LI)